

## Magnetic orientation of Ni in Zn-Ni ferrites studied by soft-x-ray magnetic circular dichroism

W. F. Pong, Y. K. Chang, M. H. Su, and P. K. Tseng

*Department of Physics, Tamkang University, Tamsui, Taiwan 251, Republic of China*

H. J. Lin, G. H. Ho, K. L. Tsang, and C. T. Chen

*Synchrotron Radiation Research Center, Hsinchu Science-based Industrial Park, Taiwan 300, Republic of China*

(Received 28 October 1996; revised manuscript received 16 January 1997)

We report the Ni  $L_{2,3}$ -edge magnetic circular dichroism (MCD) measurements of ferrimagnetic  $\text{Zn}_x\text{Ni}_{1-x}\text{Fe}_2\text{O}_4$  ( $x=0.0, 0.26, 0.50,$  and  $0.75$ ). The Ni MCD asymmetry ratio was found to decrease with increasing  $x$ , showing a reduction of the Ni average magnetic moment with Zn content. This observation is interpreted in terms of the variations in the Yafet-Kittel-type canted angles of the Ni moment, giving new insight into the superexchange interactions involving the Ni ions. A comparison with the non-Ni-specific neutron scattering and Mössbauer studies is given. [S0163-1829(97)10217-X]

$\text{Zn}_x\text{Ni}_{1-x}\text{Fe}_2\text{O}_4$  is a ferrimagnetic compound which exhibits interesting doping-dependent magnetic properties. The saturation magnetization and the critical temperature (i.e., Néel temperature) have been found to change with the Zn content and a Yafet-Kittel (YK) type canting<sup>1</sup> of the local moments has been proposed to account for these observations.<sup>2,3</sup> Neutron-diffraction,<sup>2</sup> magnetization,<sup>4</sup> and Mössbauer studies<sup>3,5</sup> have provided valuable magnetic information for this system. Mössbauer measurements suggested that the Fe magnetic moments are distributed over two different sites of the spinel structure of Zn-Ni ferrites, namely, the tetrahedral  $A$  sites and the octahedral  $B$  sites. Site-preference calculations<sup>6</sup> and neutron-diffraction measurements<sup>2</sup> on the bulk system pointed out that  $\text{Zn}^{2+}$  ions strongly prefer the  $A$  sites while the  $\text{Ni}^{2+}$  ions occupy the  $B$  sites. Hence, the cation distribution in the Zn-Ni ferrites can be expressed as  $(\text{Zn}_x\text{Fe}_{1-x})[\text{Ni}_{1-x}\text{Fe}_{1+x}]\text{O}_4$ , where the parentheses and brackets denote the  $A$  and  $B$  sites, respectively. However, the results of extended x-ray-absorption fine-structure (EXAFS) studies on a similar thin-film  $\text{Zn}_{0.16}\text{Ni}_{0.15}\text{Fe}_{2.69}\text{O}_4$  sample, which found  $\text{Ni}^{2+}$  ions occupy both  $A$  and  $B$  sites with a preference for  $B$  sites.<sup>7</sup> Recently, we have performed the O  $K$ -edge x-ray-absorption near-edge structure (XANES) spectra and first-principles spin-unrestricted calculations to investigate the degree of the  $p-d$  hybridization effects between the oxygen  $2p$  and magnetic ions  $3d$  with Zn concentration  $x$  in the bulk  $\text{Zn}_x\text{Ni}_{1-x}\text{Fe}_2\text{O}_4$  compounds.<sup>8</sup> The magnetic properties of this system are believed to be dictated by the superexchange couplings between the magnetic ions via the mediating oxygen (O) anions. Although all superexchange interactions ( $AA$ ,  $AB$ , and  $BB$ ), the predominant type of exchange mechanism between the magnetic ions, favor antiparallel alignments of the spins, the strongest  $AB$  interaction overcomes the others, resulting in parallel alignment among spins in  $A$  sites and among those in  $B$  sites.<sup>9</sup> Despite the number of experiments and theories which have been proposed to account for the magnetic properties of this system, the role of  $\text{Ni}^{2+}$  ions is still not fully understood. For example, whether the  $\text{Ni}^{2+}$  moments have the YK-type canting and how the  $AB$  and

$BB$  superexchange couplings are modified when substituting the  $B$ -sites  $\text{Fe}^{3+}$  ions by  $\text{Ni}^{2+}$  are still open questions. The neutron-diffraction data allow one to deduce only the total moment of the  $\text{Fe}^{3+}$  and  $\text{Ni}^{2+}$  ions in the  $B$  sites while the Mössbauer measurements provide information only for the  $\text{Fe}^{3+}$  ions. Due to the lack of an element-specific magnetic probe for Ni, direct information concerning the  $\text{Ni}^{2+}$  ions in the  $B$  sites has not been sufficiently reported so far.<sup>10</sup>

To help understand the role of  $\text{Ni}^{2+}$  ions in the magnetic couplings in the Zn-Ni ferrites, Ni-specific magnetization measurements using the soft-x-ray magnetic circular dichroism (MCD) technique were performed. The Ni MCD asymmetry ratio was found to decrease with increasing Zn content, suggesting that YK-type canting, proposed previously for the Fe moment in Zn-Ni ferrites, also occurs for the Ni moment. The dependency of the canted angles of Ni and Fe moments on the Zn content were found to be slightly different, indicating that there are differences in the superexchange interactions when substituting the  $B$ -site  $\text{Fe}^{3+}$  ions by  $\text{Ni}^{2+}$  ions. A comparison with the results obtained from earlier neutron-diffraction and Mössbauer studies will also be given.

The measurements were performed at the AT&T Bell Laboratories Dragon beamline at the National Synchrotron Light Source (NSLS) using the x-ray-absorption spectroscopic (XAS) technique. The beamline set up in the circular polarization mode has been described previously.<sup>11</sup> In these measurements, the photon energy resolution was set at  $\sim 0.4$  eV in the 840–890 eV range, and the degree of circular polarization was set at 77%. An alternating magnetic field of 1.2 KOe was applied parallel to the sample surface, and the grazing angle of the incident light was fixed at  $30^\circ$  with respect to the sample surface. The absorption spectra were obtained at room temperature by monitoring the soft-x-ray fluorescence yield with a high-sensitive seven-element germanium detector. The energy scales of the spectra were calibrated using the well-known spectrum of a  $\text{CaF}_2$  thin film. The sample preparations, x-ray-diffraction characterization, and the chemical analysis of the  $\text{Zn}_x\text{Ni}_{1-x}\text{Fe}_2\text{O}_4$  ( $x=0.0, 0.26, 0.5,$  and  $0.75$ ) samples used in these studies have already been reported.<sup>5</sup> The samples were ground using ceramic tools, sieved to a fine powder (particle size  $< 400$

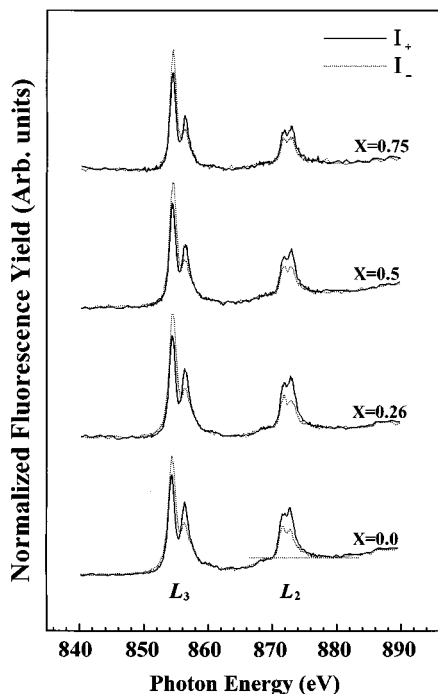


FIG. 1. Normalized Ni  $L_{2,3}$ -edge fluorescence yield x-ray-absorption spectra of  $Zn_xNi_{1-x}Fe_2O_4$  at room temperature.

mesh) and rubbed onto an adhesive tape and placed in the ultrahigh-vacuum system. All measurements were performed at room temperature.

Figure 1 shows the photon-flux-normalized Ni  $L_{2,3}$ -edge XAS spectra of  $Zn_xNi_{1-x}Fe_2O_4$  ( $x=0.0, 0.26, 0.5$ , and  $0.75$ ). The  $I_+$  ( $I_-$ ) is the absorption spectrum taken with the projection of the spin of the incident photons parallel (antiparallel) to the spin direction of the Ni  $3d$  majority electrons. The two white line regions, labeled  $L_3$  and  $L_2$  in Fig. 1, are the electron transitions from the Ni  $2p_{3/2}$  and  $2p_{1/2}$  core levels to the Ni  $3d$  unoccupied states, respectively.<sup>12</sup> The MCD spectrum, e.g.,  $I_+ - I_-$ , is shown in Fig. 2. In contrast to the single-peak feature observed at the  $L_3$  and  $L_2$  absorption white lines of metallic Ni,<sup>12</sup> rather complicated XAS and MCD spectra were observed, exhibiting strong multiplet and crystal-field effects.<sup>13</sup> The line shapes of the XAS and MCD spectra of  $Zn_xNi_{1-x}Fe_2O_4$  samples were found to be nearly identical throughout the range of  $x$  values, except for their MCD asymmetry ratio, i.e.,  $(I_+ - I_-)/(I_+ + I_-)$ . Since the MCD asymmetry ratio is proportional to the magnetic moment averaged over different sites and magnetic orientations, a quantitative evaluation of the asymmetry ratio can provide direct information on the Ni relative average magnetic moment as a function of Zn content. Among the various spectral regions from which one can calculate the asymmetry ratio, the  $L_2$  white line region is the best choice. This is because the main peak at  $\sim 855$  eV in the  $L_3$  white line region suffers seriously from self-absorption and saturation artifacts due to its large absorption cross section; it is also very difficult to isolate the positive MCD signal of the satellite peak at  $\sim 857$  eV from the negative MCD signal of the main peak. After the removal of a linear background from the  $L_2$  white line (see the dashed straight line in Fig. 1), the XAS intensities between 870.9 and 875.6 eV were integrated separately

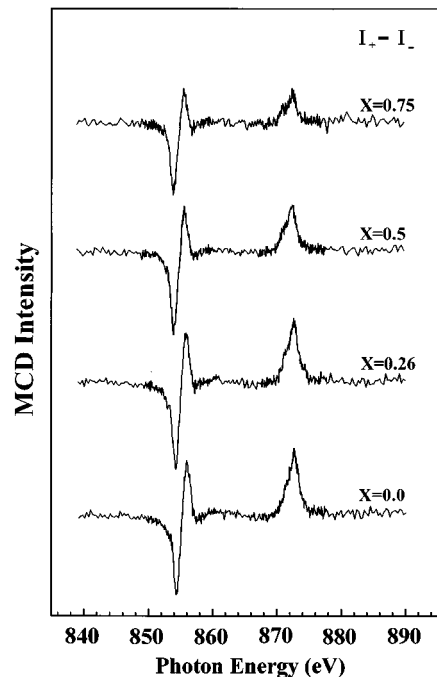


FIG. 2. Ni  $L_{2,3}$ -edge magnetic circular dichroism of  $Zn_xNi_{1-x}Fe_2O_4$ .

for the  $I_+$  and  $I_-$  spectrum. The asymmetry ratios thus obtained are 0.2241, 0.2241, 0.1926, and 0.1413 for the  $x=0, 0.26, 0.5$ , and  $0.75$  samples, respectively, showing a progressive reduction of the Ni average magnetic moment with Zn doping over a certain threshold. Ultimately, this phenomena can be interpreted as a noncollinear magnet moment arrangement, proposed for Zn-Ni ferrites by Yafet and Kittel.<sup>1</sup> For simple ferrites such as  $MFe_2O_4$  ( $M=Mn, Co$ , and  $Ni$ ), the  $M^{2+}$  substitutes the  $Fe^{3+}$  octahedral  $B$  sites and leaves the  $Fe^{3+}$  octahedral  $B$  sites intact. Regardless of whether the intrasublattice coupling (between magnetic moments in octahedral and tetrahedral sites) is ferromagnetic or antiferromagnetic, the magnetic moments of  $M^{2+}$  or  $Fe^{3+}$  in the octahedral sites are parallel to one another, i.e., Néel collinear spin arrangement,<sup>14</sup> just as the magnetic moments  $m_A$  in the  $Fe^{3+}$  tetrahedral  $A$  sites are. Upon Zn doping of the  $NiFe_2O_4$ , however, Yafet and Kittel proposed that a splitting of the octahedral sites into two subsites (labeled  $B$  and  $B'$ ) occurs, making the magnetic moments  $m_B$  in the two subsites equal in magnitude but canted by an angle of  $\theta_{YK}$  with respect to the direction of their combined moment as shown in Fig. 3. The resultant combined magnetic moment of the octahedral sites ( $Fe^{3+}$  or  $Ni^{2+}$ ) is still collinear with, but antiparallel to, that of the tetrahedral  $Fe^{3+}$  sites. By adopting this interpretation, we can relate the observed reduction of the average Ni moments to an increase in  $\theta_{YK}$ . If we assume that  $\theta_{YK}=0$  for  $x=0$ , then  $\theta_{YK}$  for any  $x$  can be calculated as  $\theta_{YK}(x) = \cos^{-1} [asy(x)/asy(0)]$ , where  $asy(x)$  is the aforementioned MCD asymmetry ratio. It shall be noted that the controversy that exists concerning the  $Ni^{2+}$  ions may occupy both  $A$  and  $B$  sites in Zn-Ni ferrites compounds according to the EXAFS results reported by Harris *et al.*,<sup>7</sup> thereby, any such evaluation using the above formula requires the confirmation of the  $Ni^{2+}$  ions which will occupy the same  $B$  sites.

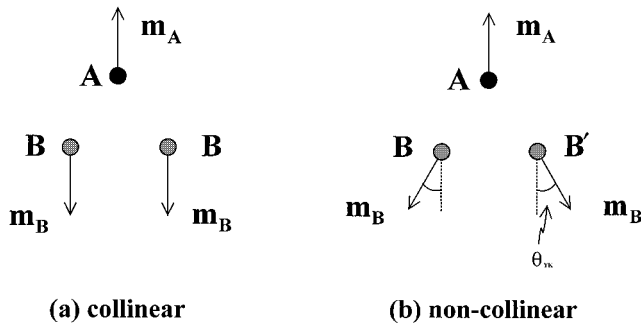


FIG. 3. Three sublattices (a) Néel collinear and (b) Yafet-Kittel noncollinear spin arrangements in Zn-Ni ferrites. The labels A, B, B' indicated the A sites and two B sites in the Zn-Ni ferrites.  $m_A$  and  $m_B$  denote the magnet moment of A sites and B sites, respectively.  $\theta_{YK}$  denote Yafet-Kittel canting angles.

An analysis of the transition-metal  $L_{2,3}$ -edge x-ray-absorption structure can obtain the characteristic information about the transition-metal ions in tetrahedral and octahedral symmetry, respectively.<sup>15</sup> In a separate study, the XAS measurements using the sample drain current mode at room temperature were performed at the Ni and Fe  $L_{2,3}$  edge on bulk  $Zn_xNi_{1-x}Fe_2O_4$  samples ( $x=0.0, 0.13, 0.25, 0.5, 0.75$ , and  $1.0$ ).<sup>16</sup> Figure 4 shows the photon-flux-normalized Ni and Fe  $L_{2,3}$ -edge x-ray-absorption spectra of  $Zn_xNi_{1-x}Fe_2O_4$ . All of the spectra shown have been scaled to the maximum of the peak heights (labeled  $a$ ). As seen in Fig. 4(a), peak  $a$  is accompanied by a lower-intensity peak (labeled  $b$ ) located just above the Ni  $L_3$  edge, while the  $L_2$ -edge white line feature exhibits a peak doublet. In contrast to Fig. 4(b), peak

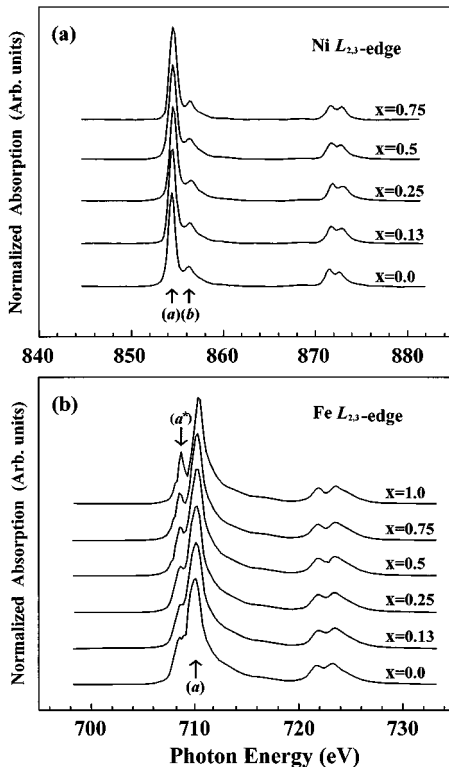


FIG. 4. Normalized Ni  $L_{2,3}$ -edge (a) and Fe  $L_{2,3}$ -edge (b) x-ray-absorption spectra of  $Zn_xNi_{1-x}Fe_2O_4$ .

$a$  at the Fe  $L_3$  edge is much broader. In particular, the split peak on the low-energy side, labeled  $a^*$  and best resolved for  $ZnFe_2O_4$  ( $x=1.0$ ), becomes progressively broader with reducing Zn content in  $Zn_xNi_{1-x}Fe_2O_4$  and appears to be least resolved for  $NiFe_2O_4$  ( $x=0.0$ ). The full width at half maximum (FWHM) of peak  $a$  at the Ni  $L_3$  edge was found to be  $\sim 0.92$  eV independent of  $x$ . On the other hand, it was increased from  $\sim 1.31$  eV at  $x=1.0$  to  $\sim 1.69$  eV at  $x=0.0$  at the Fe  $L_3$  edge. Similarly, the widths of the white line are larger for the Fe  $L_2$  edge in comparison to that for Ni  $L_2$  edge. Since the core-hole lifetime broadening of the white lines for Ni and Fe  $L_3$ -edge ( $L_2$ -edge) spectra is 0.3 and 0.2 eV (0.52 and 0.37 eV), respectively,<sup>17</sup> the broader white lines observed in the Fe spectra are not due to the core-hole lifetime but can be attributed to  $Fe^{3+}$  ions occupying both A and B sites. Upon substitution of Zn by Ni, part of the  $Fe^{3+}$  ions move from B sites to A sites. In other words, the  $Fe^{3+}$  A site to B site occupation ratio depends strongly on the Zn content. This is clearly reflected in the Fe  $L_{2,3}$ -edge XAS spectra, which contains an absorption characteristic of  $Fe^{3+}$  ions in both tetrahedral and octahedral symmetry, causing the broadening of  $a$  and  $a^*$  with decreasing Zn concentration. On the other hand, the FWHM of peak  $a$  of the Ni spectra were found to be nearly identical for different  $x$ , showing that the  $Ni^{2+}$  ions occupy only the B sites. This conclusion is consistent with the results of neutron diffraction measurements<sup>2</sup> and site-preference calculations.<sup>6</sup> The EXAFS studies found  $Ni^{2+}$  ions occupying both A and B sites in the thin-film Zn-Ni ferrites system, one possible explanation for this discrepancy may be due to the differences of the raw materials between the bulk and thin-film used and/or the procedures used to prepare the samples.<sup>7</sup>

We now discuss the MCD asymmetry ratio in relation to the  $\theta_{YK}$  of the Ni magnetic moments. Referring to the equation of  $\theta_{YK}(x) = \cos^{-1} [\text{asy}(x)/\text{asy}(0)]$  and introducing the value of asymmetry ratio which were already obtained, the  $\theta_{YK}$  of the Ni magnetic moments thus determined are  $0^\circ, 0^\circ, 31^\circ$ , and  $51^\circ$  for  $x=0, 0.26, 0.5$ , and  $0.75$  samples, respectively. Figure 5 compares the  $\theta_{YK}$  of the Ni moment determined from our MCD measurements with those obtained from neutron diffraction<sup>2</sup> and Mössbauer measurements.<sup>3</sup> Since the neutron-diffraction data allow one to deduce only the total moment of the  $Fe^{3+}$  and  $Ni^{2+}$  ions in the B sites, on the other hand, the Mössbauer technique measures only the Fe moments; the  $\theta_{YK}$  determined thus are attributed to the YK canting of the Fe moments. The  $\theta_{YK}$  vs  $x$  plot of the Ni moment exhibits similar characteristics to that of the Fe moment as well as the average of the Fe and Ni moment, i.e., a monotonous increase in  $\theta_{YK}$  for Zn content above a threshold value, the reduction in the net Ni moment due to the presence of  $\theta_{YK}$  thus demonstrates that YK-type canting also occurs for the Ni magnetic moments. More interestingly, the threshold Zn content for the Ni moments seems to be lower than that for the Fe moments, and the  $\theta_{YK}$  are larger for Ni than for Fe. Leung *et al.*<sup>3</sup> interpreted the reason for the  $\theta_{YK}$  determined by the neutron-diffraction method will be larger than that determined by Mössbauer spectroscopy. An explanation based on the relative strength of the  $Fe^{3+}(B)-Fe^{3+}(A)$  exchange interactions are about three times larger than that of the  $Ni^{2+}(B)-Fe^{3+}(A)$  interactions,

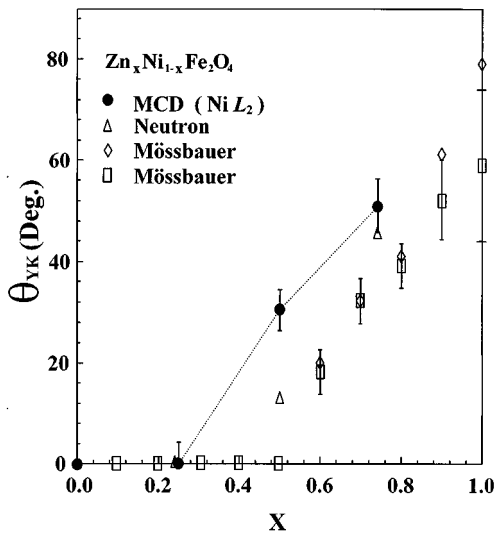


FIG. 5. Yafet-Kittel canting angles,  $\theta_{YK}$ , as a function of Zn content,  $x$ , from different magnetic measurements of  $Zn_xNi_{1-x}Fe_2O_4$ . The dashed line serves only as a visual guide for the MCD data (●). (△) represents data from the neutron-diffraction method (Ref. 2). (□) and (◇) represent data from Mössbauer studies (Ref. 3).

since the strength of the exchange interaction is strongly influenced by the value of  $\theta_{YK}$  in these compounds.<sup>2</sup> As a consequence of this conclusion, it follows that the average canting angle of the average  $\theta_{YK}$  of  $Ni^{2+}(B)$  ions will be qualitatively greater than that of  $Fe^{3+}(B)$  ions; therefore, just as expected, the  $\theta_{YK}$  angle determined with the Ni-specific MCD spectra will be larger than that determined with the Mössbauer spectroscopy, and the  $\theta_{YK}$  angle deduced from the neutron-diffraction method is just an intermediary between the two mentioned techniques, which agrees well with our results as shown in Fig. 5. Furthermore, one reasonably believes that the increase in the  $\theta_{YK}$  of magnetic ions means that a decrease in the overlap of the wave functions between two nearest-neighboring magnetic ions as well as that between magnetic ions and oxygen anions, leads to a reduction in superexchange interactions occurring between the magnetic ions and mediated by the intervening oxygen anions. It is interesting to look at the trend of O  $2p$  magnetic ion  $3d$  hybridization effects to associate the variation  $\theta_{YK}$  of magnetic ions with Zn content. In an earlier O  $K$ -edge XANES study of  $Zn_xNi_{1-x}Fe_2O_4$ ,<sup>8</sup> we found that the two distinct pre-edge features vary systematically as a function of the Zn content in these compounds. The decreases in the intensity of pre-edge features with the increase  $x$  indicates that Zn substitution reduces couplings of the O  $2p$  orbitals with the magnetic ion  $3d$  orbitals. Strictly speaking, it reveals that, as the concentration of Zn is increased, the intensity of pre-edge features is more or less constant up to  $x$

$=0.25$ , beyond which they *decrease* monotonously as shown in Fig. 2 of Ref. 8, exhibiting opposite characteristics to that of YK-type canting angle  $\theta_{YK}$  of magnetic ions, i.e., a monotonous *increase* in  $\theta_{YK}$  for Zn content above a threshold value as shown in Fig. 5. The results support the hypothesis that the variations of  $\theta_{YK}$  are strongly associated with the hybridization effects between O  $2p$  and magnetic ion  $3d$  orbitals in Zn-Ni ferrites. It is also worth noting that there is a difference in threshold Zn content for the Ni moments seem to be lower than that for the Fe moments, this implies that the influence of Zn doping on the superexchange coupling is different for Ni-O-Fe/Ni as compared to Fe-O-Fe/Ni. While the above explanations regard quantitatively magnitudes of  $\theta_{YK}$  for the Ni moments and that for the Fe moments, some possible effects shall also be taken into account for  $\theta_{YK}$ . Due to the reason that there is not only a difference in the meaning of magnetization as determined which has already been mentioned, but also the effect of the external magnetic field applied,<sup>18</sup> the measured temperature (Mössbauer data were taken at 7 K), the random distributions, and the equal moments of the  $Ni^{2+}$  and  $Fe^{3+}$  ions in  $B$  sites, respectively. Nevertheless, we would like to point out that our results concerning the  $\theta_{YK}$  angles, as shown in Fig. 5, provide new evidence that the Néel-type collinear ordering of  $Ni^{2+}$  ions is occurring on  $B$  sites when the Zn content is below near  $x=0.26$ . While the critical Zn substitution, the YK-type of the spin arrangement also developed for  $Ni^{2+}$  ions increases linearly as a function of Zn content in Zn-Ni ferrites. Such a technique will also be applied further to the more complicated case of Fe  $L_{2,3}$ -edge MCD spectra. Ideally, it is possible to use this technique individually to determine the orientation of the Fe moment in Zn-Ni ferrites; however, one shall face a task due to the fact that  $Fe^{3+}$  ions align antiferromagnetically and may provide no net magnetic moment.

In summary, we have shown that the (Zn-content-dependent) absorption measurements contain information on the magnetization of the  $Ni^{2+}$  ions in octahedral  $B$  sites, and that the MCD spectra reflect directly the orientation of the Ni magnetic moment in Zn-Ni ferrites. This allows one to independently determine the YK-type canting angle and magnetic properties for  $Ni^{2+}$  ions, even when the composition has  $Ni^{2+}$  and  $Fe^{3+}$  ions at the same  $B$  sites in Zn-Ni ferrites.

One of the authors (W.F.P.) acknowledges support by the National Science Council of the Republic of China under Contract No. NSC86-2613-M-032-004. The Ni  $L_{2,3}$ -edge MCD measurements were performed at the AT&T Bell Laboratories Dragon beamline at the NSLS and the separate Ni and Fe  $L_{2,3}$ -edge x-ray-absorption spectra were measured at the high-energy spherical grating monochromator (HSGM) beamline at the Synchrotron Radiation Research Center (SRRC).

- <sup>1</sup>Y. Yafet and C. Kittel, *Phys. Rev.* **87**, 290 (1952).
- <sup>2</sup>N. S. Satya Murthy, M. G. Natera, S. I. Youssef, R. J. Begum, and C. M. Srivastava, *Phys. Rev.* **181**, 969 (1969).
- <sup>3</sup>L. K. Leung, B. J. Evans, and A. H. Morrish, *Phys. Rev. B* **8**, 29 (1973).
- <sup>4</sup>G. K. Joshi, A. Y. Khot, and S. R. Sawant, *Solid State Commun.* **65**, 1593 (1988).
- <sup>5</sup>T. M. Uen and P. K. Tseng, *Phys. Rev. B* **25**, 1848 (1982).
- <sup>6</sup>J. Smit and H. P. J. Wijn, *Ferrites* (Wiley Interscience, New York, 1959).
- <sup>7</sup>V. G. Harris, N. C. Koon, C. M. Williams, O. Zhang, M. Abe, and J. P. Kirkland, *Appl. Phys. Lett.* **68**, 2082 (1996).
- <sup>8</sup>W. F. Pong, M. H. Su, M. H. Tsai, H. H. Hsieh, J. Y. Pieh, Y. K. Chang, K. C. Kuo, P. K. Tseng, J. F. Lee, S. C. Chung, C. I. Chen, K. L. Tsang, and C. T. Chen, *Phys. Rev. B* **54**, 16 641 (1996).
- <sup>9</sup>C. Kittel, *Introduction to Solid State Physics* (Wiley, New York, 1986), p. 439.
- <sup>10</sup>The preliminary results of this study have been published in *Physica B* **208&209**, 781 (1995).
- <sup>11</sup>C. T. Chen and F. Sette, *Rev. Sci. Instrum.* **60**, 1616 (1989); C. T. Chen, *ibid.* **46**, 1023 (1992).
- <sup>12</sup>C. T. Chen, F. Sette, Y. Ma, and S. Modesti, *Phys. Rev. B* **42**, 7262 (1990); C. T. Chen, N. V. Smith, and F. Sette, *ibid.* **43**, 6785 (1991).
- <sup>13</sup>G. van der Laan and B. T. Thole, *Phys. Rev. B* **43**, 13 401 (1991).
- <sup>14</sup>L. Néel, *Ann. Phys. (N.Y.)* **3**, 137 (1948).
- <sup>15</sup>F. M. F. de Groot, J. C. Fuggle, B. T. Thole, and G. A. Sawatzky, *Phys. Rev. B* **42**, 5459 (1990); G. van der laan and I. W. Kirkman, *J. Phys. Condens Matter* **4**, 4189 (1992).
- <sup>16</sup>W. F. Pong *et al.* (unpublished).
- <sup>17</sup>See *Unoccupied Electron States*, edited by J. C. Fuggle and J. E. Inglesfield (Springer-Verlag, Berlin, 1992), Appendix B.
- <sup>18</sup>J. Piekoszewski, L. Dabrowski, and J. Suwalski, *Solid State Commun.* **16**, 75 (1975).